ORIGINAL ARTICLE

Number of P-Wave Fragmentations on P-SAECG Correlates with Infiltrated Atrial Fat

Sindhoora Murthy, B.S.,* Patricia Rizzi, M.D.,† Nathan Mewton, M.D., Ph.D.,† David G. Strauss, M.D., Ph.D.,‡ Chia Y. Liu, Ph.D.,† Gustavo Jardim Volpe, M.D.,† Francis E. Marchlinski, M.D.,§ Peter Spooner, Ph.D.,† Ronald D. Berger, M.D., Ph.D.,† Peter Kellman, Ph.D.,¶ Joao A.C. Lima, M.D.,† and Larisa G. Tereshchenko, M.D., Ph.D.†

*From the *Whiting School of Engineering, Johns Hopkins University, Baltimore, MD; †The Division of Cardiology, Department of Medicine, Johns Hopkins University School of Medicine, Baltimore, MD; ‡Food and Drug Administration, Silver Spring, MD; §Hospital of the University of Pennsylvania, Philadelphia, PA; and ¶National Institutes of Health, National Heart, Lung, and Blood Institute, Bethesda, MD*

Background: Although atrial fibrillation (AF) triggers are known, the underlying AF substrate is less well understood. The goal of our study was to explore correlations between electrophysiological and structural characteristics of atria in patients with paroxysmal AF and individuals at AF risk.

Methods: Patients in sinus rhythm (N = 90; age 57 ± 10 year; 55 men [63.2%]) with structural heart disease and paroxysmal AF (n = 12 [13%]), or with AF risk factors and LVEF > 35% (n = 78), underwent SAECG and cardiac magnetic resonance study. Interatrial and epicardial fat was analyzed with a Dark-blood DIR-prepared Fat-Water-separated sequence in the horizontal longitudinal axis. All local P-wave extrema were identified on SAECG leads during sinus rhythm. A P-wave fragmentation (P_f) was defined as an absolute difference between adjacent extrema which was above three standard deviations of noise, and was normalized by the duration of the P wave in the corresponding lead.

Results: The P_f was greater on the filtered than on the unfiltered P-SAECG signal (13.1 ± 3.8 vs. 3.4 ± 1.2; P < 0.0001). P_f was the greatest on the Y lead (13.0 ± 3.5 on Y lead vs. 12.1 ± 3.4 on Z lead; P = 0.003. P_f on Z lead correlated with interatrial fat index (r = 0.544; P = 0.001). Epicardial fat significantly correlated with body mass index (BMI; r = 0.302; P = 0.015). After adjustment for BMI, left atrium (LA) size, epicardial fat, and interatrial septum width, interatrial fat independently associated with the P_f on Z lead (β-coefficient 0.009 [95%CI 0.0003–0.019]; P = 0.043).

Conclusions: Infiltrated atrial fat correlates with discontinuous conduction on posterior LA wall and represents AF early substrate.

Ann Noninvasive Electrocardiol 2014;19(2):114–121

atrial fibrillation; P-SAECG; cardiac magnetic resonance; infiltrated atrial fat

An estimated 2.23 million people in the United States have diagnosed atrial fibrillation (AF).[1] AF increases the risk of stroke and death[2,3] and leads to important socioeconomic consequences such as chronic disease management, disability, and increased hospital admissions. Moreover, the AF burden is increasing because of the aging US population since AF tends to be more prevalent in the elderly.[4,5] Although our understanding of AF pathophysiology has significantly advanced over the last two decades, the treatment of AF is rarely curative, and in many cases AF progresses from

Address for correspondence: Larisa G. Tereshchenko, M.D., Carnegie 568, 600 N. Wolfe St., Baltimore, MD 21287; Fax: 410-614-8039; E-mail: lteresh1@jhmi.edu. Phone: 410-502-2796

Financial support & relationships with industry: Study was partially supported by Cardiac Translational Research Implementation Program (C-TRIP) grant from NIH/National Heart, Lung and Blood Institute #P20HL101397 and the Leducq Foundation.

Clinical Trial Registration: *NCT01353131*

DOI:10.1111/anec.12084

paroxysmal AF to persistent AF.[6] The development of a strategy for the primary prevention of AF is urgently needed. However, the substrate and the mechanisms of early AF genesis are not fully understood.

Underlying structural heart diseases, such as coronary heart disease, hypertensive heart disease, valvular heart disease, cardiomyopathy, and heart failure (HF), predispose patients to AF.[7] Atrial fibrosis[8] is associated with clinically manifest AF. Epicardial fat was shown associated with AF.[9,10] In the Framingham Heart Study epicardial fat was associated with prevalent AF.[11] Experiments showed paracrine properties of epicardial fat and release of proinflammatory and profibrotic substances.[12] At the same time, autopsy studies demonstrated that fat can infiltrate myocardium.[13] However, infiltrated atrial fat has not been previously studied in vivo in patients with paroxysmal AF and in individuals at risk of AF. Only recent technology to quantify in vivo infiltrated myocardial fat became available.[14]

Electrophysiologic studies have shown that an abnormally prolonged and fractionated A-EGM, which is a sign of delayed and nonuniform conduction through the atria, is characteristic of patients with AF.[15,16] Modeling studies have shown that A-EGM fractionation is a measure of fibrosis and discontinuous conduction.[17] Abnormally prolonged P waves on signal-averaged electrocardiograms (P-SAECGs) predicted AF paroxysms in HF patients[18] and patients after cardiac surgery.[19] Still, very few studies have explored atrial electrophysiological properties and atrial structural characteristics in patients at risk of AF, without clinically manifest AF. We hypothesized that number of P-wave fragmentations on P-SAECG correlates with infiltrated atrial fat and represents early substrate of AF.

METHODS

Study Population

We present the results of analysis of a baseline visit of an ongoing prospective observational cohort study of patients with structural heart disease without overt systolic HF (NCT01353131). Study protocol was approved by the Johns Hopkins Institutional Review Board, and all study participants gave written, informed consent upon entering the study. Study design was reported previously.[20,21] Study included patients of the Johns Hopkins Hospital with structural heart disease, who have had a 12-lead ECG recorded between October 1, 2009 and March 31, 2010. Patients younger than 21 and older than 70 years, with left ventricular (LV) systolic dysfunction (LV ejection fraction [EF] $\leq$ 35%), having chronic renal insufficiency with estimated glomerular filtration rate $\leq$ 30 mL/min, and contraindication to contrast-enhanced CMR were excluded.

P-Wave ECG Analysis

A standard 12-lead ECG and SAECG (MAC 5000, GE Medical Systems, Milwaukee, WI, USA) was recorded at rest. Cardioactive drugs were not withdrawn before the ECG recording. Orthogonal XYZ leads were continuously recorded with 1000 Hz sampling rate and 1 μV amplitude resolution. Ectopic atrial and ventricular beats were eliminated and 350 clean sinus beats were collected, aligned, and averaged. Averaged signals for the X, Y, and Z leads were also combined into a vector sum, which was calculated as the Euclidean norm of the X, Y, and Z leads. An ECG Research Workstation, Hires Module (GE Marquette Medical Systems) was used to translate the proprietary file format and extract unfiltered, averaged X, Y, and Z leads, and the vector sum of the X, Y, and Z leads.

Custom-made software running on MATLAB R 2012a for Mac OS X (The MathWorks, Inc., Natick, MA, USA) was developed. The ECG signal was filtered using a bandpass 40–300 Hz filter. The averaged P wave on the unfiltered X, Y, and Z leads, filtered X,Y, and Z leads, the unfiltered vector sum, and filtered vector sum were analyzed by two investigators (SM, LT), blinded to the CMR results. Unfiltered and filtered P-wave duration on each lead was measured (Fig. 1).

P Fragmentations

P fragmentations (P_f) were measured on unfiltered X, Y, and Z leads, filtered X, Y, and Z leads (bandpass 40–300 Hz filter, using zero phase filtering), and the vector sum (Euclidean norm) of the filtered and unfiltered X, Y, and Z leads. First, the baseline noise level was measured on the segment from the end of the T wave to the beginning of the P wave. The noise threshold (3SD) was individually determined for

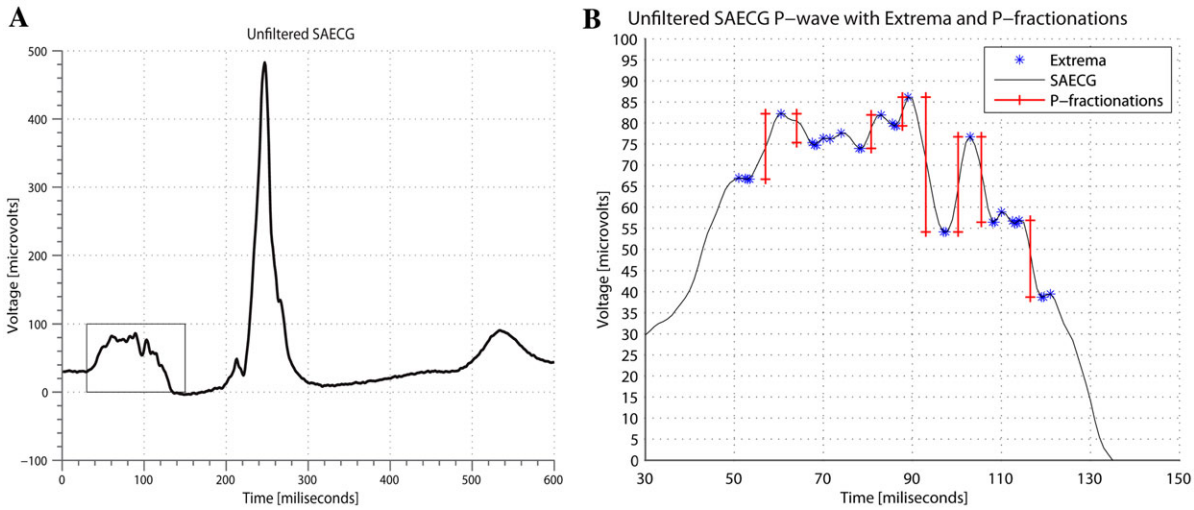

Figure 1. P wave fragmentations measurement. (A) Representative example of SAECG, with the P wave outlined in the rectangle; (B) P wave further zoomed into the rectangular section. All of the local extrema are shown by stars, and the thresholded P fragmentations, are shown by vertical lines.

each set of data. Local extrema were defined to be those points whose voltages were either strictly greater or less than both the previous and consequent data points. The voltage differences between adjacent local extrema were calculated. If such a difference exceeded predefined 3SDs noise threshold, a P fragmentation was detected. The number of P fragmentations, average width, and height of the P fragmentations were calculated. The P fragmentations were then normalized by the P-wave duration of corresponding lead, per 100 ms of the duration of the P wave. The ECG shown in Figure 1 represents a patient's SAECG signal, as well as the detection of the differences in adjacent extrema (stars) and the detection of the P fragmentations (vertical lines).

Atrial CMR Analysis

Patients underwent CMR with a 1.5-T scanner (Siemens Healthcare, Avanto, Erlangen, Germany) on the same day as the ECG recordings. All CMR analyses were performed on dedicated workstations with ARGUS (Siemens Healthcare, Malvern, PA, USA). All analyses were performed by three experienced observers who were blind to the results of the ECG analysis (NM, PR, CL). The endocardial and epicardial borders of the LV were outlined at end-diastole and end-systole on short-axis cine images. The papillary muscles were included in the LV end-diastolic volume (LVEDV) and left ventricular end-systolic volume (LVESV), and were excluded from the LV mass. Left ventricular ejection fraction (LVEF), LVEDV and LVESV were calculated using Simpson's rule. LV mass was determined by the sum of the myocardial areas in the end-diastolic phase. LVEDV, LVESV, and LV mass were normalized by body surface area (BSA), and respective indices calculated. BSA was calculated using the Mosteller equation. It was previously shown that BSA impacts left atrium (LA) size parameters.[22] Total area of the LA and right atrium (RA) were measured and normalized by BSA as well.

A representative example of a patient's image from our CMR analysis is presented in Figure 2. The presence of interatrial fat was assessed with a Dark-blood DIR-prepared Fat-Water-separated sequence[14;23] in the horizontal longitudinal axis (four-chamber view). An OsiriX DICOM viewer (Geneva, Switzerland) was used to quantify the area of the structure of interest. The width of the cephaled portion of the interatrial septum was measured in this study at the level of the fossa ovalis, as described by Shirani et al.[24] Interatrial fat area was measured, and normalized by BSA. Epicardial fat area was measured in the horizontal longitudinal axis only, and was normalized by BSA as well.

Statistical Analysis

Statistical analysis was computed using STATA 12 (StataCorp LP, College Station, TX, USA).

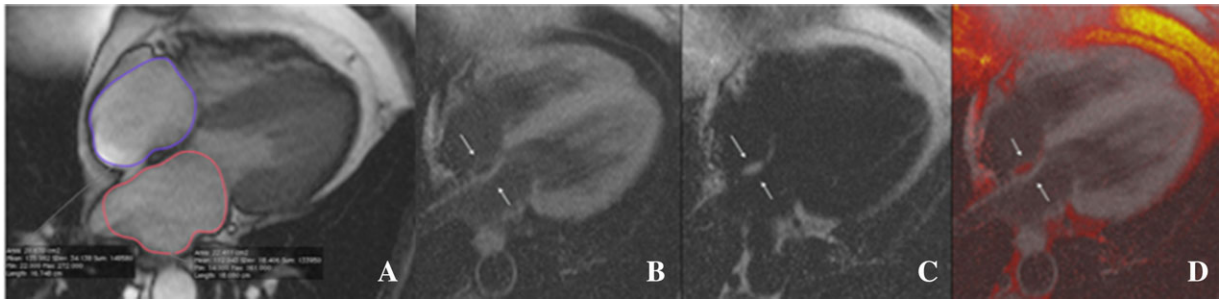

Figure 2. Cardiac magnetic resonance fat image. Representative example of Fat-Water DB IR GRE sequence. For the same patient as above, (A) HLA cine MRI during atrial diastole showing left and right atria areas measurement. The bottom row shows the Dark-blood DIR-prepared-Fat-Water-separated sequences. (B) "Water image"- fat signal is suppressed (C) "Fat image" the water signal is suppressed. (D) Fused image (fat and water images added). A cushion of fat deposit in the atrial septum is seen in black in the water image, white in the fat image and black in the fused image (white arrows).

We first explored the distribution of each of our variables. Distribution of interatrial fat and interatrial fat index variables were skewed, and therefore, these variables were log-transformed before entering further analyses. Paired *t*-test was used to compare atrial electrophysiological parameters measured on different ECG leads (XYZ), and to compare parameters measured on filtered and unfiltered ECG signal. The results are presented as mean ± SD. Categorical variables were compared by Pearson's chi-square test. Pairwise correlations were studied between normally distributed variables. Multiple linear regression analysis was performed to determine the predictors of electrophysiological atria characteristic of slow discontinuous conduction P_f. Structural atrial parameters (LA area index, interatrial septum width, epicardial fat index, and log-transformed interatrial fat) were adjusted by the body mass index (BMI) in this multiple linear regression model.

Table 1. Clinical Characteristics of Study Participants

Characteristic	N = 90
Age (SD), year	59.1 (9.3)
Females, n (%)	32 (35.5)
Whites, n (%)	34 (37.9)
Hypertension, n (%)	63 (70)
Hypertension Hx (SD), year	9.9 (7.3)
Diabetes mellitus, n (%)	(22.2)
Diabetes mellitus Hx (SD), year	8.3 (6.2)
Body mass index (SD), kg/m^2	31.0 (15.1)
History of MI, n (%)	17 (18.9)
History of PCI/CABG, n (%)	19 (21.1)
NYHA class ≥ II, n (%)	23 (25.6)
Systolic blood pressure (SD), mmHg	147.7 (22.2)
Diastolic blood pressure (SD), mmHg	87.7 (12.7)
eGFR, mL/min	64.6 (2.3)
Glucose (SD), mg/dL	119.8 (49.6)
Beta-blockers, n (%)	12 (13.3)
ACE-I/ARBs, n (%)	35 (38.9)
TZD, n (%)	19 (21.1)
Ca antagonists, n (%)	30 (30.0)
Statins, n (%)	52 (57.8)
Current or former smoker, n (%)	45 (50.0)

RESULTS

Study Population

The study population consisted of 90 patients. The mean age was 57 ± 10 years. Slightly more than half of the study population was comprised of men (n = 55 [61%]), and whites (n = 53 [59%]). At the same time, the mean LVEF was normal (60.5 ± 9.0), and most of the participants had NYHA class I HF (n = 67 [74%]). Clinical characteristics of the study participants are presented in Table 1. The routine 12-lead ECG parameters and the heart chambers size parameters were within normal range (Table 2).

Comparison of Electrophysiological Characteristics

The P_f was greater on the filtered than on the unfiltered P-SAECG signal (13.1 ± 3.8 vs. 3.4 ± 1.2; $P < 0.0001$). All of the parameters that were observed were more pronounced on the Y lead (Table 2). P_f was the greatest on the Y lead (13.0 ± 3.5 on Y lead vs. 12.1 ± 3.4 on Z lead; $P = 0.003$), and P_f was the smallest on the X lead (11.0 ± 3.3 on X lead vs. 13.0 ± 3.5 on Y lead; $P = 0.0003$). Differences in the number of unfiltered P_f mirrored the differences in the number of filtered

Table 2. Electrophysiological and Structural Parameters of the Heart Atria and Ventricles

Characteristic	N = 90
P duration (SD), ms	112.0 (13.1)
PQ interval (SD), ms	176.9 (32.6)
Heart rate (SD), bpm	65.7 (10.4)
QRS duration (SD), ms	101.6 (21.6)
P-axis (SD), deg	48.3 (32.1)
QTc duration (SD), ms	429.0 (24.5)
X lead P_f, n/100 ms	3.2 (1.2)
Y lead P_f, n/100 ms	4.4 (1.9)
Z lead P_f, n/100 ms	3.1 (1.4)
$X_{40–300\ Hz}$ P_f, n/100 ms	11.0 (3.3)
$Y_{40–300\ Hz}$ P_f, n/100 ms	13.0 (3.5)
$Z_{40–300\ Hz}$ P_f, n/100 ms	12.1 (3.4)
$SAECG_{40–300\ Hz}$ P_f, n/100 ms	13.2 (1.2)
LVEF (SD; %)	60.5 (9.0)
LV mass index (SD), g/m^2	66.9 (17.7)
LVESVI (SD), mL/m^2	27.8 (11.4)
LVEDVI (SD), mL/m^2	67.7 (16.6)
Right atrium area index (SD), cm^2/m^2	9.1 (2.8)
Left atrium area index (SD), cm^2/m^2	10.5 (2.4)
Epicardial fat index (SD), cm^2/m^2	7.5 (2.4)
Epicardial fat (SD), cm^2	14.6 (5.7)
Interatrial fat index (SD), cm^2/m^2	0.23 (0.26)
Interatrial fat (SD), cm^2	0.46 (0.53)
Atrial septum width (SD), cm	0.52 (0.25)

P_f. The width of filtered P_f was similar in all leads (6.3 ± 1.3 ms on X lead vs. 6.3 ± 1.4 ms on Y lead, vs. 6.4 ± 1.3 ms on Z lead; NS). At the same time, the width of unfiltered P_f was different across the ECG leads. The widest unfiltered P_f were seen on X lead (25.9 ± 10.2 ms on X lead vs. 19.8 ± 9.0 ms on Y lead; $P < 0.0001$), and the narrowest unfiltered P_f were noticed on the Y lead (19.8 ± 9.0 ms on Y lead vs. 23.3 ± 8.8 ms on Z lead; $P = 0.0006$). Amplitude of both filtered and unfiltered P_f similarly differed across the X, Y, and Z leads. The largest P_f amplitude was observed on Y lead (46.5 ± 22.3 μV on Y lead vs. 40.4 ± 19.1 μV on Z lead; $P = 0.036$) and the smallest P_f amplitude was measured on X lead (35.6 ± 19.0 μV on X lead vs. 46.5 ± 22.3 μV on Y lead; $P = 0.0006$).

Correlations between Electrophysiological Characteristics and Atrial Structures

P_f moderately strongly positively correlated with interatrial fat index (Fig. 3): the larger interatrial fat area, the higher the P_f on the Z lead was. Interatrial fat area did not correlate with BMI, whereas epicardial fat significantly correlated with BMI ($r = 0.302$; $P = 0.015$).

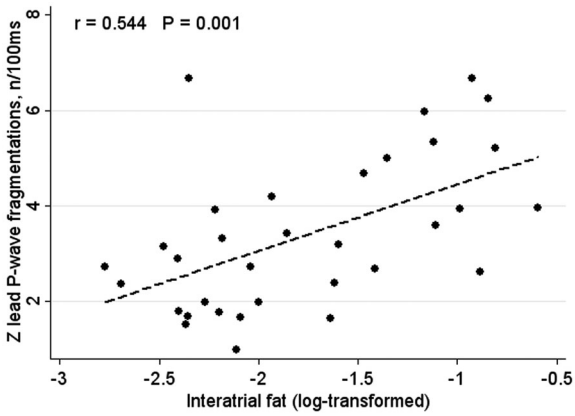

Figure 3. Correlations between the number of P fragmentations and interatrial fat. Scatter plot of the number of P fragmentations, normalized by P wave width (n/100 ms) on Z SAECG lead (Y) against log-transformed interatrial fat (X).

To determine which heart atrial structures affected the characteristics (width, amplitude) of the P fractionations, we ran multiple regression analyses, separately for P_f on X, Y, and Z leads. Size of LA, width of interatrial septum, interatrial and epicardial fat, and BMI, were included in each multiple linear regression model. Only interatrial fat (log-transformed) independently positively associated with the number of P_f on Z lead (Table 3), but not on other ECG leads.

DISCUSSION

In this study, we showed that infiltrating interatrial fat was independently associated with the number of P_f on Z SAECG lead in patients with paroxysmal AF and individuals at risk of AF. Although P_f on Y SAECG lead were larger and more numerous, as compared to P_f on other ECG leads, only Z lead P_f significantly correlated with interatrial fat, which underscores importance of the posterior atrial wall in the development of electrophysiological AF substrate at an early stage, and suggests that P_f on Z lead reflects discontinuous conduction on the posterior LA wall. Importantly, interatrial fat was a significant predictor of P_f on the Z SAECG lead after adjustment for LA area index, atrial septum width, BMI, and epicardial fat.

Table 3. Multiple Linear Regression Model Predicting the Number of P_f on Z Lead

Predictor	β Coefficient (95% CI)	P Value
Epicardial fat index (cm^2/m^2)	−0.0021 (−0.0049 to 0.00073)	0.141
Log-transformed interatrial fat	0.009 (0.0003 to 0.019)	0.043
Atrial septum width (cm^2/m^2)	−0.005 (−0.031 to 0.020)	0.671
Left atrium area index (cm^2/m^2)	−0.001 (−0.0007 to 0.0010)	0.296
Body mass index (kg/m^2)	0.0001 (−0.0008 to 0.0010)	0.770

Infiltrated Interatrial and Epicardial Fat: Role in AF

The role of epicardial fat in the AF development has been previously shown. The epicardial adipose tissue was shown to secrete proinflammatory cytokines (tumor necrosis factor-alpha, interleukin-1, interleukin-6),[25] as well as anti-inflammatory substances.[26] Kourliouros et al.[27] showed that an increase in the adiponectin release from epicardial fat was associated with freedom from AF after cardiac surgery.

Recent advancement in imaging modalities established that the epicardial fat volume of the entire heart is independently associated with AF.[11,28] Large clusters of epicardial adipose tissue, adjacent to the posterior LA wall,[29] anterior roof, LA appendage, and lateral mitral isthmus[10] were described in AF patients. Epicardial fat volume and the location of the fat were both associated with the sites of high dominant frequency or complicated fractionated A-EGMss during AF.[30] Shin et al.[31] showed that AF patients had significantly larger periatrial epicardial adipose tissue thickness and larger width of interatrial septum as measured by multislice computer tomography.

However, little attention was paid to another important feature of a fatty heart—the fatty deposits in the atrial septum and infiltration of endocardium and mid-myocardium by adipocytes.[24,28] Pathology studies[24,28] showed that fatty deposits in the atrial septum are proportional to the volume of the epicardial heart and correlate with history of atrial arrhythmia, including AF and conduction abnormalities (sinoatrial and atrioventricular block). Massive fatty deposits in the atrial septum ($\geq$ 2 cm) served as a marker of adipose tissue infiltrates in the RV myocardium, and the endocardium of RA, LA, RV, and LV. Even after excision of epicardial fat in such hearts, adipose tissue comprised 30–50% of the cardiac weight at necropsy.[28] Kellman et al. recently developed methodology of in vivo imaging of the infiltrated interatrial fat,[14,23] which was used in this study. Our study underscored the importance of infiltrated interatrial fat imaging and quantification, and for the first time demonstrated association between infiltrated interatrial fat and discontinuous LA conduction. We speculate that infiltrated atrial fat precedes development of atrial fibrosis and characterizes early preclinical AF substrate. Further prospective studies are needed to test this hypothesis.

Atrial Electrophysiology, Characterized by P-SAECG

The signal averaging technique in ECG analysis was introduced nearly 40 years ago.[32,33] Multiple studies have shown that prolonged P-SAECG duration is associated with AF.[34,35] Various technical approaches were considered for characterization of P-wave SAECG duration[19] and atrial late potentials.[36] For example, a lower root mean square voltage of the last 20 ms of the P wave (RMS 20) was shown linked with AF.[37] At the same time, invasive electrophysiological studies revealed that a fractionated A-EGM during sinus rhythm is typical for paroxysmal AF.[16] Tanigawa et al.[16] defined quantitative criteria for abnormal A-EGM as duration of A-EGM $\geq$ 100 ms and/or $\geq$8 fragmented deflections. However, the quantification of P fragmentations was not previously implemented on P-SAECG. In this study, we normalized the number of P fragmentations by the duration of P wave on the corresponding SAECG lead to refine the SAECG metric, analogous to the fractionated intracardiac A-EGM. In our study, P_f characteristics on the Z SAECG lead provided the most meaningful results. Such local expression of P_f is explained by the relationship between the axis of SAECG lead and the sum LA axis, and is consistent with what has been previously reported in literature.[38,39] Since P-wave duration on SAECG may change dramatically under different states of the autonomic nervous system,[40] quantification of P fragmentations on Z lead might become a

valuable marker to complement P-SAECG duration for risk stratification of AF, and as a surrogate for non-invasive assessment of fractionated A-EGM. Future studies are needed to test this hypothesis.

We speculate that P_f on Z SAECG lead characterizes discontinuous conduction on the posterior wall of the LA. However, this hypothesis should be further tested. Moreover, it is important to emphasize that results of our study should be interpreted carefully. Observed association between P fragmentations and interatrial fat has moderate strength. Therefore, other, unmeasured in our study factors (e.g. LA fibrosis, ganglionated plexuses activity) could be responsible for P_f appearance on P-SAECG.

LIMITATIONS

Several limitations of this study should be considered. Small study population did not allow us to fully characterize nonlinear relationships between P fragmentations and LA structures. Our study is cross-sectional and is not a prospective observational study, which would be potentially needed to establish and confirm a cause–effect relationship. Furthermore, we did not measure the fat volumetrically. There is no doubt that the absence of volumetric measurement of epicardial fat in this study imposed significant limitation for quantification of epicardial fat, which, however, was not the goal of the study. At the same time, the approach of quantification of infiltrated interatrial fat on a longitudinal four-chamber view provided a certain advantage. Results of our study suggest that quantification of interatrial fat in a single view might be sufficient for detection and quantification of infiltrated adipose tissue in the atria. In such case area of interatrial fat in the septum serves as a marker of the degree of the general intra-atrial fat infiltration. This opens a new avenue for potentially wide implementation of the proposed approach in routine CMR procedure. However, additional studies have to be conducted first to test this hypothesis.

CONCLUSION

Infiltrating interatrial fat is independently associated with the number of P-wave fragmentations on Z SAECG lead, likely reflecting discontinuous conduction on the posterior wall of the LA. Further study of normalized by P-SAECG width P fragmentations is warranted. Infiltrating interatrial fat and P fragmentations characterize AF substrate in patients with paroxysmal AF and individuals with structural heart disease at risk of AF early in the structural heart disease continuum.

REFERENCES

1. Feinberg WM, Blackshear JL, Kronmal R, et al. Prevalence, age distribution, and gender of patients with atrial fibrillation. Arch Intern Med 1995;155:469–473.
2. Wolf P, Abbott RD, Kannel WB. Atrial fibrillation as an independent risk factor for stroke: The Framingham Study. Stroke 1991;22(8):983–988.
3. Benjamin EJ, Wolf PA, Agostino RBD, et al. Clinical Investigation and Reports Impact of Atrial Fibrillation on the Risk of Death The Framingham Heart Study. Circulation 1998;98:946–952.
4. Furberg CD, Psaty BM, Manolio TA, et al. Prevalence of atrial fibrillation in elderly subjects (the Cardiovascular Health Study). Am J Cardiol 1994;74(3):236–241.
5. Benjamin EJ, Wolf PA, D'Agostino RB, et al. Impact of atrial fibrillation on the risk of death: The Framingham Heart Study. Circulation 1998;98(10):946–952.
6. Iwasaki YK, Nishida K, Kato T, et al. Atrial fibrillation pathophysiology: Implications for management. Circulation 2011;124(20):2264–2274.
7. Krahn AD, Manfreda J, Tate RB, et al. The natural history of atrial fibrillation: incidence, risk factors, and prognosis in the manitoba follow-up study. The Am J Med 1995;98:476–484.
8. Teh AW, Kistler PM, Lee G, et al. Long-term effects of catheter ablation for lone atrial fibrillation: Progressive atrial electroanatomic substrate remodeling despite successful ablation. Heart Rhythm 2012;9(4):473–480.
9. Al Chekakie MO, Welles CC, Metoyer R, et al. Pericardial fat is independently associated with human atrial fibrillation. J Am Coll Cardiol 2010;56(10):784–788.
10. Tsao HM, Hu WC, Wu MH, et al. Quantitative analysis of quantity and distribution of epicardial adipose tissue surrounding the left atrium in patients with atrial fibrillation and effect of recurrence after ablation. Am J Cardiol 2011;107(10):1498–1503.
11. Thanassoulis G, Massaro JM, O'Donnell CJ, et al. Pericardial fat is associated with prevalent atrial fibrillation/clinical perspective. Circ Arrhythm Electrophysiol 2010;3(4):345–350.
12. Venteclef N, Guglielmi V, Balse E, et al. Human epicardial adipose tissue induces fibrosis of the atrial myocardium through the secretion of adipo-fibrokines. Eur Heart J 2013 Mar 22 [Epub ahead of print].
13. Tansey DK, Aly Z, Sheppard MN. Fat in the right ventricle of the normal heart. Histopathology 2005;46(1):98–104.
14. Kellman P, Hernando D, Shah S, et al. Multiecho dixon fat and water separation method for detecting fibrofatty infiltration in the myocardium. Magn Reson Med 2009;61(1):215–221.
15. Cosio FG, Palacios J, Vidal JM, et al. Electrophysiologic studies in atrial fibrillation. Slow conduction of premature impulses: A possible manifestation of the background for reentry. Am J Cardiol 1983;51(1):122–130.
16. Tanigawa M, Fukatani M, Konoe A, et al. Prolonged and fractionated right atrial electrograms during sinus rhythm in patients with paroxysmal atrial fibrillation and sick sinus node syndrome. J Am Coll Cardiol 1991;17(2):403–408.

17. Jacquemet V, Henriquez CS. Genesis of complex fractionated atrial electrograms in zones of slow conduction: a computer model of microfibrosis. Heart rhythm 2009;6(6):803–810.
18. Yamada T, Fukunami M, Shimonagata T, et al. Prediction of paroxysmal atrial fibrillation in patients with congestive heart failure: A prospective study. J Am Coll Cardiol 2000;35(2):405–413.
19. Steinberg JS, Zelenkofske S, Wong SC, et al. Value of the P-wave signal-averaged ECG for predicting atrial fibrillation after cardiac surgery. Circulation 1993;88:2618–2622.
20. Mewton N, Rizzi P, Strauss D, et al. Screening for Arrhythmogenic myocardial substrate by 12-Lead ECG QRS Score, QRS-T angle, late potentials and T-wave alternans. J Am Coll Cardiol 2012;59(13):E737.
21. Strauss DG, Mewton N, Verrier RL, et al. Screening entire health system ECG databases to identify patients with arrhythmogenic myocardial substrate at increased risk of death. Circulation 2011;124(21):A552.
22. Maceira AM, Cosin-Sales J, Roughton M, et al. Reference left atrial dimensions and volumes by steady state free precession cardiovascular magnetic resonance. J Cardiovasc Magn Reson 2010;12:65. doi:10.1186/1532-429X-12-65
23. Kellman P, Hernando D, Arai AE. Myocardial fat imaging. Curr Cardiovasc Imaging Rep 2010;3(2):83–91.
24. Shirani J, Roberts WC. Clinical, electrocardiographic and morphologic features of massive fatty deposits ("lipomatous hypertrophy") in the atrial septum. J Am Coll Cardiol 1993;22(1):226–238.
25. Mazurek T, Zhang L, Zalewski A, et al. Human epicardial adipose tissue is a source of inflammatory mediators. Circulation 2003;108(20):2460–2466.
26. Iacobellis G, Barbaro G. The double role of epicardial adipose tissue as pro- and anti-inflammatory organ. Horm Metab Res 2008;40(7):442–445.
27. Kourliouros A, Karastergiou K, Nowell J, et al. Protective effect of epicardial adiponectin on atrial fibrillation following cardiac surgery. Eur J Cardiothorac Surg 2011;39(2):228–232.
28. Shirani J, Berezowski K, Roberts WC. Quantitative measurement of normal and excessive (cor adiposum) subepicardial adipose tissue, its clinical significance, and its effect on electrocardiographic QRS voltage. Am J Cardiol 1995;76(5):414–418.
29. Batal O, Schoenhagen P, Shao M, et al. Left atrial epicardial adiposity and atrial fibrillation. Circ Arrhyth Electrophysiol 2010;3(3):230–236.
30. Nagashima K, Okumura Y, Watanabe I, et al. Does location of epicardial adipose tissue correspond to endocardial high dominant frequency or complex fractionated atrial electrogram sites during atrial fibrillation? Circ Arrhythm Electrophysiol 2012;5(4):676–683.
31. Shin S, Yong H, Lim H, et al. Total and interatrial epicardial adipose tissues are independently associated with left atrial remodeling in patients with atrial fibrillation. J Cardiovasc Electrophysiol 2011;22(6):647–655.
32. Berbari EJ, Lazzara R, El-Sherif N, et al. Extracardiac recordings of His-Purkinje activity during conduction disorders and junctional rhythms. Circulation 1975;51(5):802–810.
33. Sadanandan S, Steinberg JS. Signal-averaged P Wave: Technique and clinical applications. Ann Noninvasive Electrocard 1999;4(4):401–407.
34. Darbar D, Hardy A, Haines JL, et al. Prolonged signal-averaged P-wave duration as an intermediate phenotype for familial atrial fibrillation. J Am Coll Cardiol 2008;51(11):1083–1089.
35. Guidera SA, Steinberg JS. The signal-averaged P wave duration: A rapid and noninvasive marker of risk of atrial fibrillation. J Am Coll Cardiol 1993;21(7):1645–1651.
36. Darbar D, Jahangir A, Hammill SC, et al. P wave signal-averaged electrocardiography to identify risk for atrial fibrillation. Pacing Clin Electrophysiol 2002;25(10):1447–1453.
37. Budeus M, Hennersdorf M, Felix O, et al. Prediction of atrial fibrillation in patients with cardiac dysfunctions: P wave signal-averaged ECG and chemoreflexsensitivity in atrial fibrillation. Europace 2007;9(8):601–607.
38. Holmqvist F, Carlson J, Waktare JE, et al. Noninvasive evidence of shortened atrial refractoriness during sinus rhythm in patients with paroxysmal atrial fibrillation. Pacing Clin Electrophysiol 2009;32(3):302–307.
39. Holmqvist F, Platonov PG, McNitt S, et al. Abnormal P-wave morphology is a predictor of atrial fibrillation development and cardiac death in MADIT II patients. Ann Noninvasive Electrocardiol 2010;15(1):63–72.
40. Cheema AN, Ahmed MW, Kadish AH, et al. Effects of autonomic stimulation and blockade on signal-averaged P wave duration. J Am Coll Cardiol 1995;26(2):497–502.